Chinese Chemical Letters 33 (2022) 4900–4903

Contents lists available at ScienceDirect

Chinese Chemical Letters

journal homepage: www.elsevier.com/locate/cclet

Simultaneous enhancement of phosphorescence and chirality by host–guest recognition of molecular tweezers

Diankun Jia[a,b], Hua Zhong[c], Sixun Jiang[c], Risheng Yao[a,b,*], Feng Wang[c,*]

[a] School of Chemistry and Chemical Engineering, Hefei University of Technology, Hefei 230009, China
[b] School of Food and Biological Engineering, Hefei University of Technology, Hefei 230009, China
[c] CAS Key Laboratory of Soft Matter Chemistry, Department of Polymer Science and Engineering, University of Science and Technology of China, Hefei 230026, China

ARTICLE INFO

Article history:
Received 23 December 2021
Revised 27 February 2022
Accepted 27 February 2022
Available online 4 March 2022

Keywords:
Host–guest chemistry
Molecular tweezer
Room-temperature phosphorescence
Chirality
Stimuli-responsiveness

ABSTRACT

A novel type of host–guest recognition systems have been developed on the basis of a Au(III) molecular tweezer receptor and chiral Pt(II) guests. The complementary host–guest motifs display high non-covalent binding affinity (K_a: ~10^4 L/mol) due to the participation of two-fold intermolecular π–π stacking interactions. Both phosphorescence and chirality signals of the Pt(II) guests strengthen in the resulting host–guest complexes, because of the cooperative rigidifying and shielding effects rendered by the tweezer receptor. Their intensities can be reversibly switched toward pH changes, by taking advantage of the electronic repulsion effect between the protonated form of tweezer receptor and the positive-charged guests in acidic environments. Overall, the current study demonstrates the feasibility to enhance and modulate phosphorescence and chirality signals simultaneously *via* molecular tweezer-based host–guest recognition.

Host–guest chemistry field has experienced a rapid growth due to the development of various synthetic receptors since the discovery of crown ethers half a centray ago [1–3]. These receptors can encapsulate guest molecules with high non-covalent binding affinity and selectivity, endowing diverse functions to the resulting supramolecular host–guest complexes [4–10]. Thereinto, promotion of luminescent efficiency *via* host–guest complexation has received considerable attention [11–17]. Liu's and Ma's groups have encapsulated phosphorescent emitters into the rigid macrocycles such as cyclodextrins and cucurbiturils [15,16]. It reduces susceptibility of triplet excitons toward environmental changes, leading to high room-temperature phosphorescent (RTP) emission intensities. Another important functionality of host–guest complexation is to create symmetry breaking and thereby amplify supramolecular chirality. The so-called supramolecular chirogenesis [18–21] occurs between achiral synthetic receptors and chiral guests (or *vice versa*), showing prospects for absolute configuration determination and asymmetric catalysis applications. Although emission or chirality enhancement of host–guest complexes has been successfully achieved, it remains unexplored to strengthen these two signals in a simultaneous manner, which would be promising for circularly polarized luminescence, multi-channel sensory, and nonlinear optical applications [22–26].

Molecular tweezers represent an important type of synthetic receptors apart from macrocycles and cages. The two flat and aromatic pincers in *syn* conformation are separated by a rigid or semi-flexible spacer, rendering an open cavity for guest encapsulation by virtue of pre-organization effect [27–29]. In recent years, molecular tweezers with metal coordination centers (termed as "metallotweezers") have attacted tremendous attention becasue of their ease of synthesis and fruitful photophysics [30–32]. In this repect, our research group has synthesized a novel metallotweezer **1** (Scheme 1), with two cofacially pincer gold(III) units tethered by a rigid diphenylpyridine spacer [24]. It is capable of sandwiching square planar platinum(II) complex **2** (Scheme 1) as the complementary guests. The heterometallic host–guest recognition not only renders rigidification effect for the triplet platinum(II) emitter, but shields it from external quenchers such as oxygen and solvent molecules, giving rise to intense yellow-colored phosphorescence for **2** in both solid and solution states.

On this basis, herein we sought to prove the generality of tweezer approach to enhance phosphorescence. Meanwhile, supramolecular chirality is induced for the metallotweezer-based host–guest complexes, by incorporating chiral elements into the Pt(II) triplet emitters. Specifically, compounds **3** and **4** (Scheme 1)

* Corresponding authors.
E-mail addresses: yaors@hfut.edu.cn (R. Yao), drfwang@ustc.edu.cn (F. Wang).

https://doi.org/10.1016/j.cclet.2022.02.081
1001-8417/

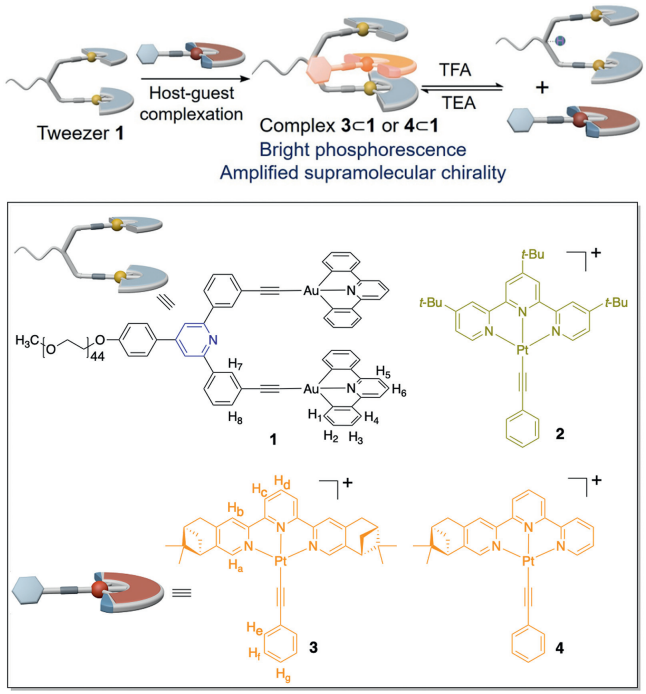

Scheme 1. Schematic representation for the enhancement and modulation of both phosphorescence and chirality signals upon host–guest recognition between Au(III) molecular tweezer **1** and the complementary Pt(II) guests **3** and **4**. The chemical structures of Au(III) tweezer receptor **1** and Pt(II) guests **2**–**4** are shown in the frame. The counteranions are tetrafluoroborate (BF_4^-) in compounds **2**–**4**.

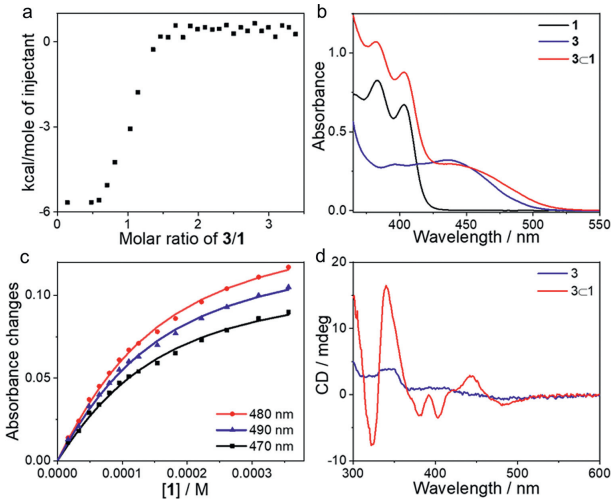

Fig. 1. (a) ITC data for titrating **3** (2.00 mmol/L in acetonitrile) into an acetonitrile solution of **1** (0.10 mmol/L). (b) UV–vis spectra of **1**, **3** and a 1:1 mixture of **1** and **3** in DMSO ($c = 0.10$ mmol/L for each compound). (c) Intensity changes of absorbance at 470 nm, 480 nm, and 490 nm upon addition of **1** (2.00 mmol/L in DMSO) into **3** (0.10 mmol/L in DMSO) at 298 K. The solid lines are obtained *via* a Matlab-based global analysis program. (d) CD spectra of **3** (blue line) and a 1:1 mixture of **1** and **3** (red line) in acetonitrile.

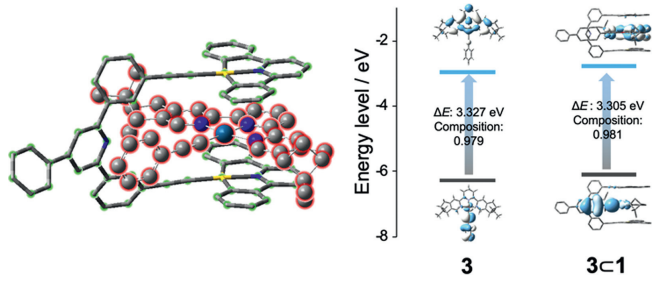

Fig. 2. Optimized geometry of complex **3⊂1** *via* DFT calculation (left), together with the energy-level diagram of **3** and **3⊂1** *via* TD-DFT computation (right). The black lines and blue lines mark the energy levels of HOMOs and LUMOs, respectively.

have been designed and synthesized (Schemes S1, S2 and Figs. S1–S6 in Supporting information), with the presence of two and one (1*R*)-pinene units [33] on the main ligands, respectively. It is expected to enhance emission and chirality signals simultaneously for the resulting complexes **3⊂1** and **4⊂1**. Moreover, the metallotweezer receptor **1** features pH-responsive pyridine unit on its rigid spacer [34]. In acidic environments, severe electronic repulsion exists between the protonated form of **1** and the positively-charged guests **3**–**4**. It triggers guest release from the cavity of metallotweezer receptor (Scheme 1), accompanied by the decline of phosphorescent emission and supramolecular chirality intensities. Overall, the current study provides an efficient way to enhance and modulate phosphorescence and chirality signals *via* molecular tweezer-based host–guest complexation.

Non-covalent host–guest complexation between Au(III) metallotweezer **1** and Pt(II) compound **3** was firstly studied *via* isothermal titration calorimetry (ITC). A negative ITC signal emerged upon progressive addition of **3** into the acetonitrile solution of **1** (Fig. 1a and Fig. S7 in Supporting information), illustrating enthalpy-driven host–guest complexation. The abrupt change in the titration curve revealed 1:1 binding stoichiometry between **1** and **3**. Fitting the exothermic isotherm data with a one-site model provided the association constant (K_a) value of $(3.39 \pm 0.21) \times 10^4$ L/mol.

Density functional theory (DFT) calculation was employed to clarify the non-covalent complexation mode. In the optimized geometry of complex **3⊂1** (Fig. 2), **3** is encapsulated into the inner cavity of metallotweezer **1** to form a 1:1 sandwiched structure. The centroid-to-plane distances between **3** and the two Au(III) pincers on **1** are determined to be 3.42 Å and 3.46 Å, respectively. Hence, two-fold intermolecular π–π stacking interactions exist between the two [Au(III)(C^N^C)] pincers on **1** and **3**. The conclusion was supported by ^{1}H NMR measurements (Fig. S8 in Supporting information). Upon adding equivalent amount of Pt(II) compound **3** into Au(III) tweezer **1**, the [Au(III)(C^N^C)] pincer protons underwent downfield shifts ($\Delta\delta = 0.08$, and 0.09 ppm for protons H_1, and H_2, respectively), while protons H_{a-d} on **3** merged into the baseline due to the non-solvation effect.

Non-covalent complexation between **1** and **3** gave rise to UV–vis spectroscopic changes. For Au(III)-based metallotweezer **1**, a vibronic structured UV–vis absorbance was present between 350 and 420 nm (Fig. 1b). With reference to the previous literatures [35,36], this band is typical for metal–perturbed $\pi \rightarrow \pi^*$ intraligand (IL) transition of the [Au(III)(C^N^C)(C≡C–R)] units. In the meantime, Pt(II) compound **3** displayed a visible-light absorbance in the range of 385–500 nm (Fig. 1b), assigning to the admixture of $d\pi(Pt) \rightarrow \pi^*(tpy)$ metal−to−ligand charge transfer (MLCT) and $\pi(C{\equiv}CR) \rightarrow \pi^*(tpy)$ ligand−to−ligand charge transfer (LLCT) transitions (Fig. 2) [37–39]. Upon mixing equimolar amounts of **1** and **3** together in DMSO, a shoulder absorption band appeared at the low-energy region (ranging between 455 nm and 530 nm, Fig. 1b). Depending on TD-DFT calculations (Fig. 2), both HOMO and LUMO of complex **3⊂1** are essentially identical to those of compound **3**, in which the HOMO is the mixture of phenylacetylene π orbital and Pt(II) $d\pi$ orbital, while the LUMO is π^* orbital of the terpyridine ligand. The results denote the negligible contribution of metallotweezer **1** to the frontier orbitals of **3⊂1**. The bathochromic absorption of **3⊂1** could be probably ascribed to the physical perturbance effect *via* non-covalent host−guest complexation.

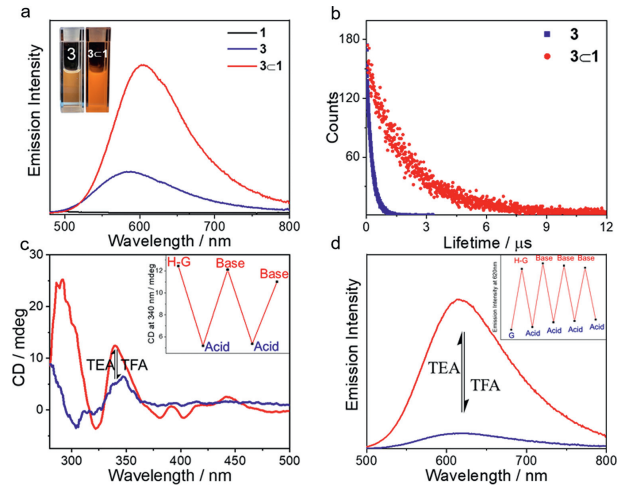

Fig. 3. (a) Emission spectra (λ_{ex} = 450 nm) of **1**, **3** and **3⊂1** in degassed acetonitrile (0.04 mmol/L for each compound). (b) Time-dependent emission lifetime decay of **3⊂1** and **3** under deaerated condition. The excited-state decay profile was fitted by a biexponential function to provide the average lifetime. Excitation wavelength was 355 nm picosecond laser. (c) CD and d) emission spectral changes of **3⊂1** (0.04 mmol/L in acetonitrile) upon the successive addition of the acetonitrile solutions of TFA and TEA (0.50 mol/L for each solution, 2 μL for each injection). Inset of c: CD intensity changes at 340 nm. Inset of d: emission intensity changes at 625 nm. "G", "H-G", "Acid", and "Base" refer to **3**, complex **3⊂1**, TFA and TEA, respectively.

On this basis, the non-covalent binding affinity of **3⊂1** was probed *via* UV–vis titration experiments. The K_a value was determined to be 1.13×10^4 (± 9.9%) L/mol, by fitting the collected UV–vis absorbances at 470, 480, and 490 nm with the global analysis method (Fig. 1c and Fig. S9a in Supporting information). The K_a values acquired by UV–vis and ITC measurements are within the same order of magnitude, validating strong non-covalent complexation strength of **3⊂1**. In view of the presence of optically active (1*R*)-pinene unit on the Pt(II) guest, CD spectroscopy was further performed for both compound **3** and complex **3⊂1**. As shown in Fig. 1d, very weak Cotton effect was detected for **3** itself. Upon adding an equimolar amount of **1** into **3**, the CD signal exhibited drastic enhancement for both low-energy MLCT/LLCT and high-energy IL transitions (positive maxima at 340 nm and 442 nm, together with negative maximum at 322 nm, $\Delta\varepsilon$ = 9.99, 1.75 and –4.64 cm^{-1} L mol^{-1}, respectively). The effective chirality transfer from the aliphatic (1*R*)-pinene to the aromatic Pt(II) pincer is attributed to the restriction of carbon–carbon and carbon–platinum bond rotations in the individual guest **3**. Accordingly, the amplified CD signal of **3⊂1** reflects the emergence of supramolecular chirality upon metallotweezer–guest complexation.

Intriguingly, the resulting host–guest complex **3⊂1** displayed emission enhancement behaviours. As shown in Fig. 3a, the metallotweezer receptor **1** was non-emissive in fluid solution [emission quantum yield (Φ_{em}) < 0.001], ascribed to the presence of thermally-accessible *d-d* or LLCT (ligand-to-ligand charge transfer) states for the Au(III) pincers [40]. Meanwhile, the Pt(II) guest **3** exhibited moderate emission in deaerated acetonitrile (λ_{max} = 583 nm, Φ_{em} = 0.07, the average lifetime τ = 0.27 μs, Figs. 3a and b). Upon mixing equimolar amounts of **1** and **3** together, an intense orange-coloured emission appeared for the mixture solution (λ_{max} = 602 nm, Fig. 3a). The Φ_{em} value of **3⊂1** was determined to be 0.61 in degassed acetonitrile, significantly higher than those of the individual compounds under the same conditions. Lifetime measurement of **3⊂1** (τ = 2.01 μs, Fig. 3b) proved the phosphorescent emission character. Notably, in aerated acetonitrile the phosphorescence quantum yield was 0.35, demonstrating the efficiency to resist oxygen upon host–guest complexation (Fig. S12 in Supporting information).

We further acquired radiative (k_r) and non-radiation (k_{nr}) decay rates of **3⊂1** to clarify the mechanism for metallotweezer-enhanced phosphorescence. In particular, the k_r and k_{nr} values of **3⊂1** were determined to be 3.03×10^5 s^{-1} and 1.94×10^5 s^{-1}, respectively. The k_r value was comparable to that of the individual guest **3** (k_r: 2.59×10^5 s^{-1}). It denotes that the Pt(II) phosphor contributes predominately to the emitting T_1 state of **3⊂1**. Meanwhile, the k_{nr} value of **3⊂1** was 18-fold lower than that of **3** (3.44×10^6 s^{-1}). We rationalized that vibrational and rotational stretching of Pt(II) phosphor is restricted to reduce non-radiative relaxations. Meanwhile, the Pt(II) triplet emitter is shielded from the polar solvents. Accordingly, it facilitates phosphorescent emission enhancement upon non-covalent host–guest complexation between **1** and **3**.

Non-covalent recognition was also examined between metallotweezer receptor **1** and Pt(II) guest **4**. Similar to that of **3⊂1**, **4** is sandwiched into the cavity of **1** with two-fold π-stacking interactions (the centroid-to-plane distances between **4** and the two Au(III) pincers on **1**: 3.43 Å and 3.52 Å, Fig. S10 in Supporting information). The K_a value of complex **4⊂1** was determined to be 1.37×10^4 (± 8.4%) L/mol on the basis of UV–vis titration measurements (Fig. S9b in Supporting information). The comparable K_a values between **4⊂1** and **3⊂1** illustrate that non-covalent host–guest binding strength is hardly influenced by the number of (1*R*)-pinene units on the Pt(II) guest structure. Complex **4⊂1** also exhibited the simultaneous enhancement of chirality and phosphorescence signals (λ_{max} = 628 nm in acetonitrile, Φ_{em}: 0.05 for **4** *versus* 0.43 for **4⊂1** in deaerated conditions, Figs. S11b and Fig. S14b in Supporting information).

It should be mentioned both complexes **3⊂1** and **4⊂1** exhibited red-shifted emission as compared to the individual Pt(II) guests. The phenomena were different from the blue-shifted emission of **2⊂1** (λ_{max}: from 589 nm of **2** to 572 nm of **2⊂1**) [24]. Generally, emission enhancement of host–guest complexes is ascribed to the synergistic shielding and rigidifying effects endowed by metallotweezer receptor **1**. In the case of complex **2⊂1**, the Pt(II) guest **2** renders large steric hindrance effect, which potentially leads to the predominance of the rigidifying effects. In comparison, the Pt(II) guests **3** and **4** possess relatively lower steric hindrance, resulting in the predominant contribution of non-covalent shielding effect. Despite the wavelength difference, the results prove the generality to enhance emission intensity of Pt(II) triplet emitters *via* metallotweezer host–guest complexation.

Next, we turned to study stimuli-responsiveness of the resulting host–guest complexes. When 2 equiv. of trifluoroacetic acid (TFA) was added, the amplified CD signals of complexes **3⊂1** in acetonitrile disappeared (Fig. 3c). Meanwhile, the visible light absorbance signal in acidic environment resembled the MLCT/LLCT absorbance of the individual compound **3** (Fig. S17 in Supporting information), suggesting pH-triggered release of the Pt(II) guest. Because of the absence of shielding and rigidifying effects rendered by the metallotweezer receptor, the intense emission at 602 nm of **3⊂1** declined significantly (Fig. 3d). The successive addition of trimethylamine (TEA) led to the re-encapsulation of Pt(II) phosphor. As a consequence, the absorption, CD, and emission bands of complex **3⊂1** recovered (Figs. 3c and d, Figs. S17a and b). The on-off switching processes were reproducible for four repeating cycles (Fig. 3d, inset). The reversible modulation of chirality and phosphorescent signals also took place for complex **4⊂1** (Figs. S17c and d).

The pH-responsive mechanism of complexes **3⊂1** and **4⊂1** was further elucidated. As can be seen, neither UV–Vis nor emission spectroscopic changes occurred for the individual compounds **3** and **4** upon adding TFA (Fig. S16 in Supporting information). Hence, the acids not function directly on the triplet emitters. We rationalized that TFA protonated metallotweezer **1**, exerting an indirect effect to modulate the optical signals of Pt(II) guests. To prove

this assertion, ^{1}H NMR measurements were performed for the control compound **5** (Fig. S15 in Supporting information). As can be seen, upon adding 2 equiv. TFA, the resonances of protons $H_{7'}$ and $H_{8'}$ underwent upfield shifts ($\Delta\delta = -0.04$ and –0.06 ppm for $H_{7'}$ and $H_{8'}$, respectively), while protons $H_{11'}$ exhibited downfield shifts (0.08 ppm). The result demonstrates protonation of diphenylpyridine unit on metallotweezer **1**, thus imparting large electronic repulsion to the positively-charged Pt(II) compounds in acidic environments.

In summary, two host–guest complexes have been successfully constructed on the basis of Au(III) tweezer **1** and chiral Pt(II) compounds **3**–**4** with high binding affinity (K_a: $\sim 10^4$ L/mol). The resulting complexes **3**⊂**1** and **4**⊂**1** exhibit orange-colored phosphorescence, with the enhancement of the emission intensities compared to the corresponding Pt(II) guests. Supramolecular chirality signals simultaneously emerged due to the restriction of free bond rotations. Both phosphorescent emission and chirality signals can be modulated toward pH changes, by taking advantage of the electronic repulsion effect between the protonated form of **1** and the positively-charged guests **3** and **4** in acidic environments. Overall, metallotweezer-based host–guest complexation provides an efficient method to enhance and modulate phosphorescence and chirality signals in a concurrent manner, which benefits the fabrication of circularly polarized phosphorescence and multi-channel sensory materials.

Declaration of competing interest

The authors declared that they have no conflicts of interest to this work.

Acknowledgments

This work was financially supported by the National Natural Science Foundation of China (Nos. 21922110 and 21871245), the Fundamental Research Funds for the Central Universities (No. WK3450000005), and the Starry Night Science Fund at Shanghai Institute for Advanced Study, Zhejiang University (No. SNZJU-SIAS-006).

Supplementary materials

Supplementary material associated with this article can be found, in the online version, at doi:10.1016/j.cclet.2022.02.081.

References

[1] Z. Liu, S.K.M. Nalluri, J.F. Stoddart, Chem. Soc. Rev. 46 (2017) 2459–2478.
[2] B. Zheng, F. Wang, S. Dong, F. Huang, Chem. Soc. Rev. 41 (2012) 1621–1636.
[3] T. Xiao, J. Wang, Y. Sheng, et al., Chin. Chem. Lett. 32 (2021) 1377–1380.
[4] L. Chen, H. Yang, Acc. Chem. Res. 51 (2018) 2699–2710.
[5] Y. Han, Z. Gao, C. Wang, R. Zhong, F. Wang, Coord. Chem. Rev. 414 (2020) 213300.
[6] Y. Deng, X. Li, C. Han, S. Dong, Chin. Chem. Lett. 31 (2020) 3221–3224.
[7] J. Wang, L. Li, W. Yang, et al., ACS Macro Lett. 8 (2019) 1012–1016.
[8] C. Qin, Y. Li, Q. Li, C. Yan, L. Cao, Chin. Chem. Lett. 32 (2021) 3531–3534.
[9] Y. Luo, W. Zhang, X. Xiao, et al., Chin. Chem. Lett. 32 (2021) 367–370.
[10] T. Feng, X. Li, J. Wu, C. He, C. Duan, Chin. Chem. Lett. 31 (2020) 95–98.
[11] R.N. Dsouza, U. Pischel, W.M. Nau, Chem. Rev. 111 (2011) 7941–7980.
[12] Y. Hou, Z. Zhang, S. Lu, et al., J. Am. Chem. Soc. 142 (2020) 18763–18768.
[13] Y. Mi, J. Ma, W. Wu, et al., J. Am. Chem. Soc. 143 (2021) 1553–1561.
[14] T. Zhang, X. Ma, H. Wu, et al., Angew. Chem. Int. Ed. 59 (2020) 11206–11216.
[15] F. Shen, Y. Chen, X. Dai, et al., Chem. Sci. 12 (2021) 1851–1857.
[16] L. Xu, L. Zou, H. Chen, X. Ma, Dyes Pig. 142 (2017) 300–305.
[17] C. Peng, W. Liang, Y. Cheng, et al., Chin. Chem. Lett. 32 (2021) 345–348.
[18] V.V. Borovkov, G.A. Hembury, Y. Inoue, Acc. Chem. Res. 37 (2004) 449–459.
[19] L. Wang, Z. Chen, W. Liu, et al., J. Am. Chem. Soc. 139 (2017) 8436–8439.
[20] J. Ji, W. Wu, L W, et al., J. Am. Chem. Soc. 141 (2019) 9225–9238.
[21] M. Liu, Y. Han, H. Zhong, X. Zhang, F. Wang, Angew. Chem. Int. Ed. 60 (2021) 3498–3503.
[22] Y. Yin, Z. Chen, Y. Han, R. Liao, F. Wang, Org. Chem. Front. 8 (2021) 4986–4993.
[23] Y. Chen, B. Sun, H. Feng, et al., Chem. Eur. J. 27 (2021) 12305–12309.
[24] Z. Li, Y. Han, F. Nie, et al., Angew. Chem. Int. Ed. 60 (2021) 8212–8219.
[25] S. Yu, Y. Wang, S. Chatterjee, F. Liang, F. Zhu, H. Li, Chin. Chem. Lett. 32 (2021) 179–183.
[26] L. Cheng, K. Liu, Y. Duan, et al., CCS Chem. 2 (2020) 2749–2763.
[27] S. Ibáñez, C. Vicent, E. Peris, Angew. Chem. Int. Ed. 61 (2022) e202112513.
[28] X. Zhao, Z. Zhao, X. Liu, X. Wu, Chin. Chem. Lett. 20 (2009) 397–400.
[29] Y.K. Tian, Y.F. Han, Z.S. Yang, F. Wang, Macromolecules 49 (2016) 6455–6461.
[30] K.M.C. Wong, V.W.W. Yam, Acc. Chem. Res. 44 (2011) 424–434.
[31] S. Ibáñez, M. Poyatos, E. Peris, Angew. Chem. Int. Ed. 56 (2017) 9786–9790.
[32] X. Zhang, Y. Han, G. Liu, F. Wang, Chin. Chem. Lett. 30 (2019) 1927–1930.
[33] X. Zhang, V. Chang, J. Liu, et al., Inorg. Chem. 54 (2015) 143–152.
[34] X. Zhang, L. Ao, Y. Han, Z. Gao, F. Wang, Chem. Commun. 54 (2018) 1754–1757.
[35] Q. Wan, J. Xia, W. Lu, J. Yang, C.M. Che, J. Am. Chem. Soc. 141 (2019) 11572–11582.
[36] A.Y.Y. Tam, K.M.C. Wong, V.W.W. Yam, J. Am. Chem. Soc. 131 (2009) 6253–6260.
[37] Y. Han, Y. Tian, Z. Li, F. Wang, Chem. Soc. Rev. 47 (2018) 5165–5176.
[38] Y. Tian, Y. Shi, Z. Yang, F. Wang, Angew. Chem. Int. Ed. 53 (2014) 6090–6094.
[39] Z. Gao, Y. Tian, H.K. Hsu, et al., CCS Chem. 3 (2021) 105–115.
[40] L.H. Doerrer, Dalton Trans. 39 (2010) 3543–3553.